Core-coupled States and Split Proton-neutron Quasiparticle Multiplets in $^{122-126}$Ag

Lalkovski, S.; Bruce, A. M.; Jungclaus, A.; Gorska, M.; Pfuetzner, M.; Caceres, L.; Naqvi, F.; Pietri, S.; Podolyak, Zs.; Simpson, G. S.; Andgren, K.; Bednarczyk, P.; Beck, T.; Benlliure, J.; Benzoni, G.; Casarejos, E.; Cederwall, B.; Crespi, F. C. L.; Cuenca-Garcia, J. J.; Cullen, I. J.; Bacelar, A. M. Denis; Detistov, P.; Doornenbal, P.; Farrelly, G. F.; Garnsworthy, A. B.; Geissel, H.; Gelletly, W.; Gerl, J.; Grebosz, J.; Hadinia, B.; Hellström, Margareta; Hinke, C.; Hoischen, Robert; Ilie, G.; Jaworski, G.; Jolie, J.; Khaplanov, A.; Kisyov, S.; Kmiecik, M.; Kojouharov, I.; Kumar, R.; Kurz, N.; Maj, A.; Mandal, S.; Modamio, V.; Montes, F.; Myalski, S.; Palacz, M.; Prokopowicz, W.; Reiter, P.

Published in:
Physical Review C (Nuclear Physics)

DOI:
10.1103/PhysRevC.87.034308

2013

Core-coupled states and split proton-neutron quasiparticle multiplets in $^{122-126}$Ag

S. Lalkovski,[1,2] A. M. Bruce,[2] A. Jungclaus,[3] M. Górska,[4] M. Pfützner,[5] L. Cáceres,[4,6,*] F. Naqvi,[4,7] S. Pietri,[4] Zs. Podolyák,[8] G. S. Simpson,[9] K. Andgren,[10] P. Bednarczyk,[4,11] T. Beck,[4] J. Benlliure,[12] G. Benzoni,[13] E. Casarejos,[14] B. Cederwall,[10] F. C. L. Crespi,[13,15] J. J. Cuenca-García,[4] I. J. Cullen,[8] A. M. Denis Bacelar,[2] P. Detistov,[16] P. Doornenbal,[4,7] G. F. Farrelly,[8] A. B. Garnsworthy,[8] H. Geissel,[4] W. Gelletly,[8] J. Gerl,[4] J. Grebosz,[4,11] B. Hadinia,[10] M. Hellström,[17] C. Hinke,[18] R. Hoischen,[17,4] G. Ilie,[7] G. Jaworski,[19,20] J. Jolie,[7] A. Khaplanov,[10] S. Kisyov,[1] M. Kmiecik,[11] I. Kojouharov,[4] R. Kumar,[21] N. Kurz,[4] A. Maj,[11] S. Mandal,[22] V. Modamio,[3,†] F. Montes,[4] S. Myalski,[11] M. Palacz,[20] W. Prokopowicz,[4] P. Reiter,[7] P. H. Regan,[8] D. Rudolph,[17] H. Schaffner,[4] D. Sohler,[23] S. J. Steer,[8] S. Tashenov,[4] J. Walker,[3,6] P. M. Walker,[8] H. Weick,[4] E. Werner-Malento,[24] O. Wieland,[13] H. J. Wollersheim,[4] and M. Zhekova[1]

[1]*Faculty of Physics, University of Sofia "St. Kliment Ohridski," Sofia 1164, Bulgaria*
[2]*School of Computing, Engineering and Mathematics, University of Brighton, Brighton BN2 4JG, United Kingdom*
[3]*Instituto de Estructura de la Materia, CSIC, E-28006 Madrid, Spain*
[4]*GSI Helmholtzzentrum für Schwerionenforschung, Planckstrasse 1, D-64291 Darmstadt, Germany*
[5]*Faculty of Physics, University of Warsaw, PL-00681 Warsaw, Poland*
[6]*Departamento de Física Teórica, Universidad Autonoma de Madrid, E-28049 Madrid, Spain*
[7]*Institut für Kernphysik, Universität zu Köln, D-50937 Köln, Germany*
[8]*Department of Physics, University of Surrey, Guildford GU2 7XH, United Kingdom*
[9]*LPSC, Université Joseph Fourier Grenoble, CNRS/IN2P3, Institut National Polytechnique de Grenoble, F-38026 Grenoble Cedex, France*
[10]*KTH Stockholm, S-10691 Stockholm, Sweden*
[11]*H. Niewodniczański Institute of Nuclear Physics, Polish Academy of Sciences, Radzikowskiego 152 Kraków 31-342, Poland*
[12]*Universidad de Santiago de Compostela, E-175706 Santiago de Compostela, Spain*
[13]*INFN Sezione di Milano, I-20133 Milano, Italy*
[14]*Universidad de Vigo, E-36310 Vigo, Spain*
[15]*Universitá degli Studi di Milano, I-20133 Milano, Italy*
[16]*Institut for Nuclear Research and Nuclear Energy, Bulgarian Academy of Science, Sofia, Bulgaria*
[17]*Department of Physics, Lund University, S-22100 Lund, Sweden*
[18]*Physik-Department E12, Technische Universität München, D-85748 Garching, Germany*
[19]*Faculty of Physics, Warsaw University of Technology, Koszykowa 75, 00-662 Warszawa, Poland*
[20]*Heavy Ion Laboratory, University of Warsaw, Pasteura 5A, 02-093 Warszawa, Poland*
[21]*Inter University Accelerator Centre, New Delhi, India*
[22]*University of Delhi, New Delhi, India*
[23]*Institute of Nuclear Research of the Hungarian Academy of Science, H-4001 Debrecen, Hungary*
[24]*IEP, Warsaw University, PL-00681 Warsaw, Poland*

(Received 18 December 2012; published 6 March 2013)

Neutron-rich silver isotopes were populated in the fragmentation of a ^{136}Xe beam and the relativistic fission of ^{238}U. The fragments were mass analyzed with the GSI Fragment Separator and subsequently implanted into a passive stopper. Isomeric transitions were detected by 105 high-purity germanium detectors. Eight isomeric states were observed in $^{122-126}$Ag nuclei. The level schemes of ^{122,123,125}Ag were revised and extended with isomeric transitions being observed for the first time. The excited states in the odd-mass silver isotopes are interpreted as core-coupled states. The isomeric states in the even-mass silver isotopes are discussed in the framework of the proton-neutron split multiplets. The results of shell-model calculations, performed for the most neutron-rich silver nuclei are compared to the experimental data.

DOI: 10.1103/PhysRevC.87.034308 PACS number(s): 21.10.Tg, 23.20.Lv, 23.35.+g, 27.60.+j

I. INTRODUCTION

The nuclear shell model [1] was introduced in the mid-20th century and its major success was the description of the magic numbers. Recently, it was suggested that for extremely neutron-rich nuclei the ordering of the orbits, and hence the magic numbers as we know them from nuclei close to the line of β stability, may change owing to diffuseness of the nuclear surface [2,3]. Further, it was pointed out that an experimental fingerprint of the changing structure may be found in the $R_{4/2}$ ratio systematics for the neutron-rich even-even nuclei, because in the case of weakening of the $\vec{l}^2$ term in the shell-model potential, the $R_{4/2}$ ratio would strongly depend on the occupation of the $\Delta j = 2$ single-particle orbits [4]. The shell quenching was also suggested to be the origin of the poor theoretical description of the r-process abundance in the region below the $A = 130$ peak [5,6].

*Present address: GANIL CAEN France.
†Present address: Istituto Nazionale di Fisica Nucleare, Laboratori Nazionali di Legnaro, Legnaro I-35020, Italy.

However, recent studies performed at GSI show no need of shell quenching to explain the structure of $^{130}_{48}Cd_{82}$ [7]. It was pointed out that if a neutron shell erosion is present in the $N = 82$ isotonic chain, it should take place deep below ^{132}Sn in the $28 \leqslant Z \leqslant 50$ proton shell. Among the candidates for strongly pronounced shell-quenching effects are the neutron-rich zirconium nuclei [3]. Of particular interest is $^{122}_{40}Zr_{82}$, which would be a magic nucleus in terms of the "classic" magic numbers. This nucleus is far from being accessible experimentally, but given that the degree of collectivity depends on the number of valence particles, a change in the neutron magic numbers would also affect the structure of the neutron midshell zirconium nuclei. To search for deviations from the midshell behavior, IBM-1 calculations were performed [8] assuming the persistence of the $N = 50$ and 82 magic numbers. The spectroscopic observables, level energies and transition strengths in $^{106}_{40}Zr_{66}$ were predicted using a Hamiltonian parametrized with respect to nuclei lying close to the line of β stability. Further, the excited states in ^{106}Zr were experimentally observed from β-decay studies performed at RIKEN [9]. The experimental level energies are in good agreement with the model predictions suggesting that $^{106}Zr_{66}$ is indeed a midshell nucleus. In ^{108}Zr [9], an isomeric decay was also experimentally observed, revealing the energy of the first excited state. It was shown that in the zirconium isotopic chain the 2^+_1 state gradually increases in energy from the midshell nucleus towards the next neutron magic number. Even though the evolution of the 2^+_1 states in the neutron-rich zirconium isotopes hints at the preservation of the "classical" magic numbers when departing from the neutron midshell ^{106}Zr nucleus, more experimental data are needed to draw firm conclusions.

A different approach to the problem is the systematic analysis of the states in the odd-mass and odd-odd nuclei and in particular the positioning of the unique-parity states relative to the normal-parity states. These high-j intruder states appear at the upper part of the shells, where low-j normal parity states are present, and are often responsible for the islands of isomerism emerging in the vicinity of the magic numbers. Also, in the odd-odd nuclei at the top of the shells, long-lived isomers emerge from the structure of the split proton-neutron multiplets [10]. Thus, the islands of isomerism in specific mass regions are directly related to the existence of the magic numbers and the identification of the opposite parity states in the odd-A and odd-odd nuclei can give a direct measure of whether the shells are quenched or not.

In the region below ^{132}Sn, the unique-parity orbits are $\pi g_{9/2}$ and $\nu h_{11/2}$ arising from the fourth proton and fifth neutron oscillator shell, respectively, leading to the appearance of positive-parity states in the odd-A ($Z = 47$) silver isotopes and states of opposite parities in the even-mass Ag nuclei. The interplay between these unique-parity and the normal-parity orbits often gives rise to isomers close to the ground state. A well-known example is $^{129}Ag_{82}$, which has a β-decaying isomer with a half-life of $t_{1/2} = 160$ ms and a 46-ms ground state [11], leading to a $^{129}Ag_{82}$ stellar half-life of the order of 80 ms. Such long-lived isomerism can shed light on the observed r-process overabundance in the $A \sim 120$ mass region. Therefore, of particular interest is the search for isomeric states in the most neutron-rich odd-mass and odd-odd nuclei, just below the doubly magic ^{132}Sn nucleus.

Prior to this study, the shell structure in nuclei around ^{132}Sn was studied in a number of experiments on isomeric decays. The ^{125,127,129}Sn nuclei were studied at LOHENGRIN [12] and during the g-RISING campaign [13]. Isomeric decay studies were performed for ^{128}Sn [14], ^{127,128,130}Cd [7,15,16], and ^{131}In [17] nuclei in the RISING Stopped beam campaign [18] and for $^{123-130}$In at LOHENGRIN [19]. The present work extends these studies towards the most neutron-rich silver nuclei.

II. EXPERIMENTAL SETUP

The neutron-rich Ag nuclei were produced during two experiments performed at GSI, Darmstadt, using the fragmentation of a ^{136}Xe beam [7,15–17] and the fission of a ^{238}U beam [20] at relativistic energies. In these experiments, the beams were accelerated to 750 MeV/A by the SIS-18 synchrotron and impinged on Be targets of 1 and 4 g/cm^2 thickness, respectively. The cocktail of fragments, produced in the fragmentation or fission, was analyzed with the GSI Fragment Separator (FRS) [21]. The ions were separated by means of their magnetic rigidities, times of flight, energy losses, and positions in the middle and final focal planes of the separator. The nuclei were slowed by an aluminum wedge-shaped degrader and implanted into a copper or plastic stopper placed at the final focal plane. Delayed γ rays were detected by the RISING multidetector array [22], comprising 105 HPGe detectors, mounted as 15 cluster detectors. The signals were digitized by Digital Gamma Finder (DGF) modules providing energy and time information.

III. EXPERIMENTAL RESULTS AND DATA ANALYSIS

A. Odd-A Ag nuclei

Prior to the current study, isomer-delayed transitions were observed in neutron-rich ^{123,125}Ag [23]. Although the low-energy transitions directly depopulating the isomeric state were not seen in that work, half-lives of $t_{1/2} = 396(37)$ ns and $t_{1/2} = 473(111)$ ns were deduced from the $\gamma(t)$ distributions of the high-energy transitions deexciting states below the isomers in ^{123}Ag and ^{125}Ag, respectively. An overall deviation of 3 keV in the γ-ray energies reported in Ref. [23] with respect to the present values is observed. Alternative level schemes from isomeric decays, were also presented in a Ph.D. thesis [24]. The present work gives revised and extended level schemes of ^{123,125}Ag, available owing to the superior efficiency of the RISING multidetector array which enables γ-ray coincidences to be clearly established. Preliminary results on the isomeric decays in ^{123,125}Ag were reported in Ref. [25], but a manuscript was not sent for the conference proceedings. During the completion of the present paper, a revised level scheme of ^{125}Ag was published in Ref. [26].

1. ^{123}*Ag*

The nucleus ^{123}Ag was produced in both experiments and observed in the FRS setting centered on the transmission of

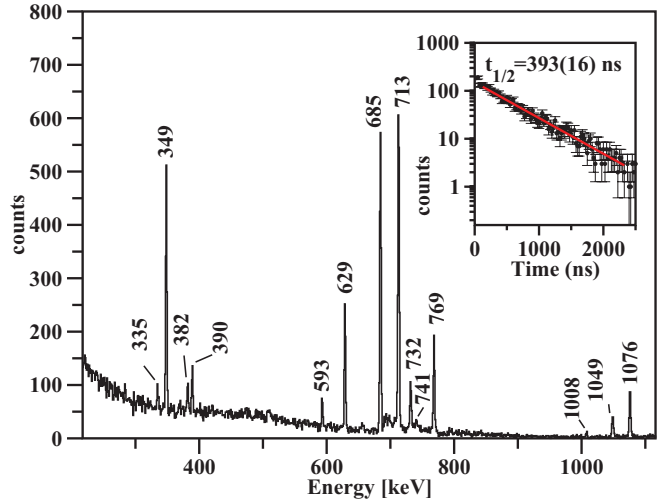

FIG. 1. (Color online) γ rays observed in delayed coincidence with ^{123}Ag ions. (Inset) A summed time spectrum for the 349-, 629-, 685-, 713-, 732-, and 769-keV transitions.

fully stripped ^{120}Rh (fission) and ^{126}Cd (fragmentation) ions, respectively.

Figure 1 shows a γ-ray spectrum observed in coincidence with ^{123}Ag ions, within a 3.75-μs-wide coincidence window opened 125 ns after the implantation. The most intense transitions, presented in Fig. 1, were previously reported and placed in level schemes [23,24]. The inset of Fig. 1 shows a summed time spectrum for the strongest transitions in ^{123}Ag. The half-life of the isomeric state $t_{1/2} = 393(16)$ ns was deduced from the fit to the slope. This value is in good agreement with 396(37) ns measured in Ref. [23] and within 2σ with 0.32(3) μs [24].

Sample coincidence spectra are shown in Fig. 2. Figure 2(a) shows that the 713-keV transition is in strong coincidence with the 685-keV transition, and in weaker coincidence with the 732-, 335-, and 349-keV transitions. In Fig. 1, the 349-keV peak is strong, while the 335-keV peak is weak, which suggests that the 349-keV transition feeds a level, which subsequently

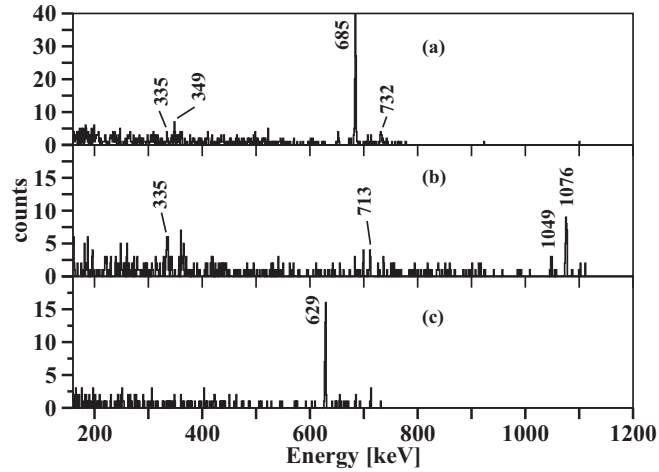

FIG. 2. ^{123}Ag γ rays, observed in coincidence with the (a) 713-keV, (b) 349-keV, and (c) 769-keV transitions, respectively.

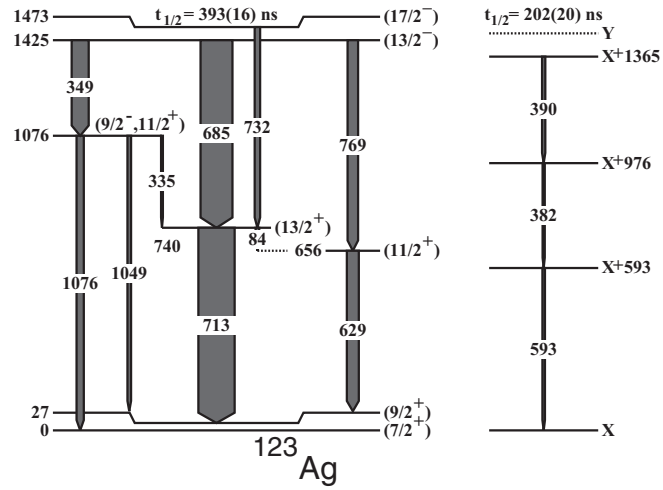

FIG. 3. Partial level scheme of ^{123}Ag, based on the γ-ray coincidences observed in the present work.

decays via a branch of transitions, some of which are parallel to the 713-keV transition. This interpretation is supported by Fig. 2(b), which shows the 349-keV line in coincidence with the 1049- and 1076-keV transitions. The 1049- and 1076-keV transitions are observed to be in mutual anticoincidence. The energy spectrum, presented in Fig. 2(c) shows a peak with an energy of 629 keV, which is in coincidence with the 769-keV γ ray. The 769- and 629-keV transitions are not observed to be in coincidence with the 713- and 685-keV transitions. In the present work, the weak 732-keV transition is observed in anticoincidence with the 685-keV transition, which suggests an ordering of the 685- and 713-keV transitions opposite to that suggested in Ref. [23]. Also, no experimental evidence was found for the 714- to 717-keV doublet reported in Ref. [23]. A level scheme based on the coincidence studies performed in the present work is shown in Fig. 3. Table I lists the γ-ray energies and intensities, as observed in the present study.

The delayed coincidence method [27] was used to estimate the half-lives of the 656-keV and 740-keV levels. It shows that the half-life of the two excited states is shorter than the DGF time binning, which is 25 ns per channel. Such a short half-life is consistent with a dipole or quadrupole nature for the 629- and 713-keV transitions.

Coincidence spectra for the weak 382-, 390-, and 593-keV transitions are shown in Fig. 4. The three γ rays are in mutual coincidence. A half-life of $t_{1/2} = 202(20)$ ns is obtained from the fit to the summed time distributions for the 382-, 390-, and 593-keV transitions. In the level scheme, this sequence is placed in parallel to the γ rays deexciting the 393-ns isomer, given that no experimental evidence was found for coincidences between the two branches.

Two weak transitions with energies of 741 and 1008 keV are also observed in coincidence with the ^{123}Ag ions, as shown in Fig. 1. Owing to the poor statistics no evidence for coincidences with the strongest γ transitions was found. However, the two unplaced transitions may be related to a weak and fragmented γ-decay branch deexciting the 1076-keV level. Such a scenario is supported by the observed intensity disbalance for the 1076-keV level.

TABLE I. Level energies (E_i), spin/parity (J^π) assignments, γ-ray energies (E_γ), and relative intensities for transitions observed in coincidence with ^{123}Ag ions.

E_i (keV)	J^π	E_γ (keV)	I_{rel} (%)
		741.2(5)[a]	4.3(7)
		1008.2(5)[a]	1.7(4)
0	$(7/2^+)$		
27	$(9/2^+)$		
656	$(11/2^+)$	629.1(5)	32.7(15)
740	$(13/2^+)$	84(1)	10(5)
		713.2(5)	100
1076	$(9/2^-, 11/2^+)$	335.2(5)	3.6(7)
		1049.3(5)	9.1(9)
		1076.3(5)	19.5(13)
1425	$(13/2^-)$	348.7(5)	42.8(14)
		684.7(5)	84.5(23)
		768.8(5)	29.5(15)
1473	$(17/2^-)$	(48)[b]	7.5[b]
		732.1(5)	15.4(11)
X			
$X+593$		593.3(5)	6.5(8)
$X+976$		382.4(5)	5.5(7)
$X+1365$		389.5(5)	8.8(9)

[a]Transition not placed in the level scheme.
[b]Transition not observed experimentally but deduced from the intensity balance at the 1425-keV level. The relative intensity is calculated assuming an $E2$ multipolarity for the 48-keV transition and $E1$ multipolarity for the deexciting transitions.

The spin and parity assignments to the states in ^{123}Ag are based on the γ-ray decay pattern, observed in the present work, and on the systematics.

$7/2^+, 9/2^+$. The systematics in Fig. 5 show that $9/2^+$ is the ground state in the $N = 50-54$ silver nuclei, while $7/2^+$ is the first excited state and $1/2^-$ is the second excited state. $7/2^+$ becomes the ground state in $^{103}_{47}Ag_{56}$ [28] and is the lowest-lying positive parity state until $^{121}_{47}Ag_{73}$ [23]. The ground state for the $N = 58-70$ silver nuclei is $1/2^-$. The $1/2^-$ level energy in the heavier silver isotopes is

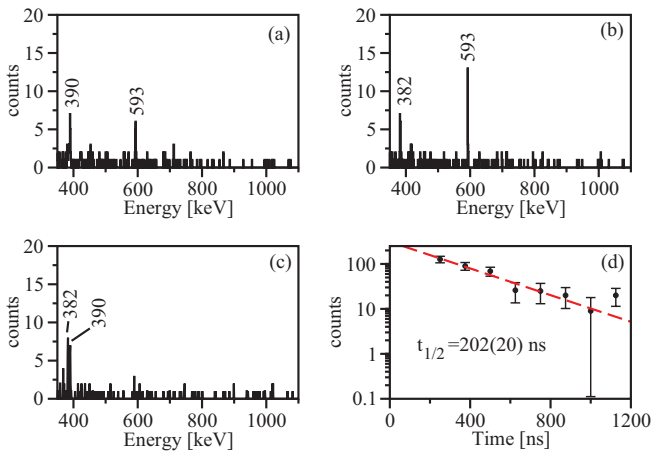

FIG. 4. (Color online) ^{123}Ag γ rays, observed in coincidence with the (a) 382-keV, (b) 390-keV, and (c) 593-keV transitions, respectively. (d) A summed time spectrum for the three transitions.

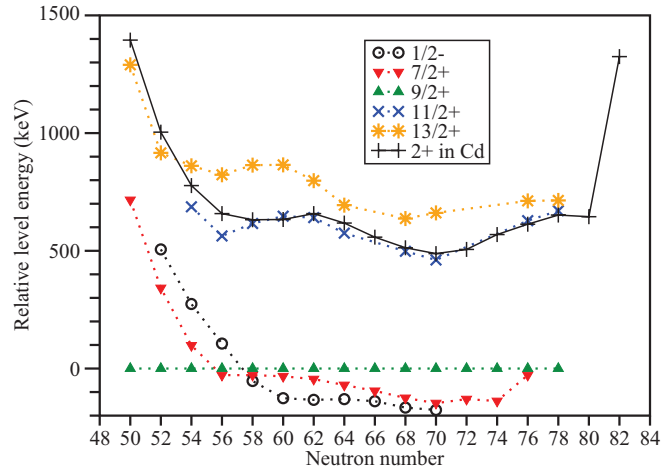

FIG. 5. (Color online) Systematics of the low-lying states in the odd-mass Ag nuclei. Level energies are plotted relative to the $9/2^+$ level energy.

unknown. Thus, based on the systematics, $1/2^-$, $7/2^+$, and $9/2^+$ are the most probable candidates for the ground state in ^{123}Ag. However, because of the strong β-decay feeding to the 264-keV $(5/2^+, 7/2^+)$ level in ^{123}Cd, the $1/2^-$ and $9/2^+$ assignments to the ground state have been ruled out [29]. Given also that the fission process populates mainly yrast states, $(7/2^+)$ is assigned to the lowest-lying state of the strongly populated sequence, deexciting the 393-ns isomer. Again, based on the systematics, $(9/2^+)$ is adopted for the 27-keV level.

$11/2^+, 13/2^+$. Figure 5 shows that the $11/2^+$ state appears at approximately 600 keV above the $9/2^+$ state and that it is correlated to the 2^+ level energies in the even-even cadmium nuclei. Also, in all silver isotopes with more than two valence neutrons outside the $N = 50$ shell closure the $11/2^+$ state is lower in energy than the $13/2^+$ state. Therefore, based on the systematics, $(11/2^+)$ and $(13/2^+)$ were assigned to the 656- and 740-keV levels, respectively. These assignments are also consistent with the dipole or quadrupole nature of the 629- and 713-keV transitions, discussed above.

$13/2^-, 17/2^-$. The 1473-keV level decays via a weak 732-keV transition to the $(13/2^+)$ state, but not to the levels with lower spin. Therefore, $J^\pi \geqslant 17/2^\pm$ can be expected for the 1473-keV state. Similarly, the 1425-keV level does not decay directly to the $(9/2^+)$ level. Therefore, a tentative $J^\pi \geqslant 13/2^\pm$ assignment can be made for this level. Furthermore, in order for the 1473-keV level to be an isomeric state, a low-energy transition is expected to compete with the 732-keV transition. Such a transition would be a 48-keV transition linking the 1473-keV level with the 1425-keV state. For a 48-keV transition of $E1$ or $E2$ nature the conversion coefficients calculated with BrIcc [30] are $\alpha(48\gamma; E1) = 1.268$ and $\alpha(48\gamma; E2) = 19.9$ and hence $B(E1) = 1.45 \times 10^{-6}$ and $B(E2) = 6.8(8)$ W.u., respectively. Both values are consistent with the hindrance factor systematics in Ref. [31], but for higher multipolarities the 48-keV transition would be enhanced from three to nine orders of magnitude and hence very unlikely. Also, the intensity balance, performed for the 1425-keV level, suggests that the 48-keV γ-ray intensity will

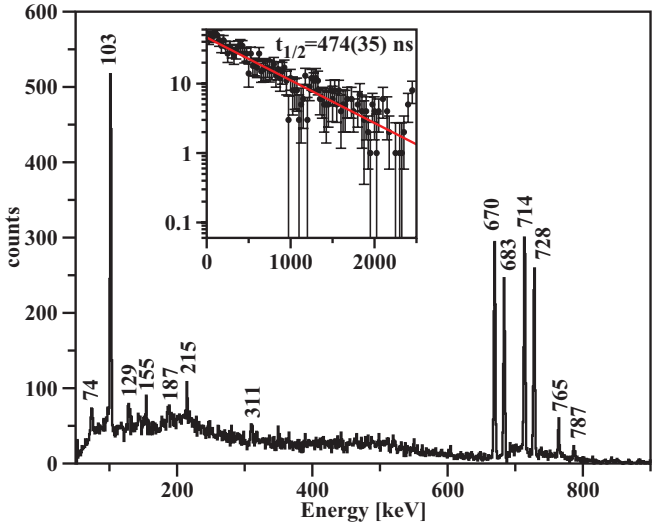

FIG. 6. (Color online) γ-ray energy spectrum, observed in coincidence with the ^{125}Ag ions. (Inset) A summed time spectrum for the 103-, 683-, and 728-keV transitions.

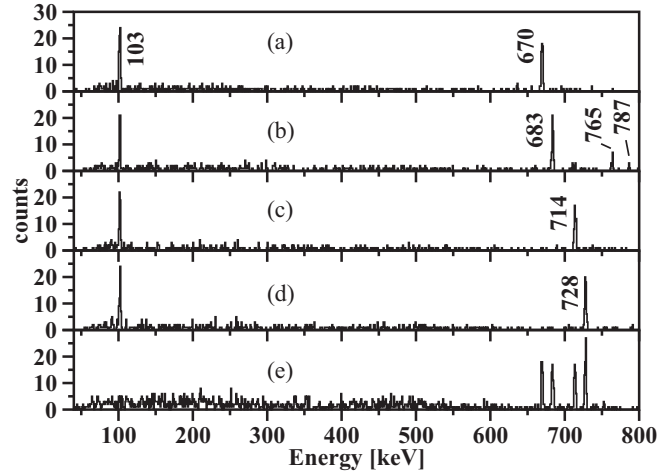

FIG. 7. ^{125}Ag γ rays, observed in coincidence with the (a) 728-keV, (b) 714-keV, (c) 683-keV, (d) 670-keV, and (e) 103-keV transitions, respectively.

be 69% of the intensity of the 713-keV transition in case of $E1$ multipolarity, and 7.5% if it is an $E2$ transition. Because, the 48-keV transition is not observed in the present experiment, $E2$ multipolarity was adopted. Hence, $J^\pi = (17/2^-)$ and $J^\pi = (13/2^-)$ assignments are made to the 1473- and 1425-keV states, respectively. Thus, assuming pure $E2$ and $M2$ nature of the isomeric transitions in ^{123}Ag, $B(E2; 17/2^- \rightarrow 13/2^-) = 6.8(8)$ W.u. and $B(M2; 17/2^- \rightarrow 13/2^+) = 1.36(12) \times 10^{-3}$ W.u. A similar isomeric decay has been observed in ^{123}In with $B(E2; 17/2^- \rightarrow 13/2^-) = 3.3(5)$ W.u. [19].

9/2⁻, 11/2⁺. Given that the 1076-keV level decays to the $(7/2^+)$ ground state and is fed by the 349-keV transition from the $(13/2^-)$ state, a $(9/2^-, 11/2^+)$ assignment to the level was made.

2. ^{125}Ag

In the present work, ^{125}Ag was observed in the ^{120}Rh FRS setting from ^{238}U fission and in the ^{130}Cd FRS setting from the fragmentation of the ^{136}Xe beam. Figure 6 shows γ rays observed in coincidence with the ^{125}Ag ions within a 3.85-μs-wide time window opened 125 ns after implantation. A group of four intense transitions at energies of approximately 700 keV and a strong 103-keV γ line is observed. Coincidence spectra are shown in Fig. 7. Figure 7(a) presents coincidences between the 103-keV and the 728-keV transitions.

The 765-keV γ rays are only in coincidence with the 714-keV γ rays, as shown in Fig. 7(b). Figure 7(c) shows coincidences between the 683- and 714-keV transitions and Fig. 7(d) shows the coincidences between 670- and 728-keV transitions. Figure 7(e) shows that the 103-keV γ rays are in coincidence with the most intense γ rays but not in coincidence with the 765- and 787-keV transitions.

The level scheme, presented in Fig. 8, is based on the coincidences observed in the present work. The energy difference between the 1501- and 1478-keV levels is 23 keV, and hence impossible to detect with the setup used. Also, because of the poor statistics, no half-life information was obtained from the time distribution of the 765-keV transition, which makes it difficult to determine whether the 1478-keV level is fed by the 1501-keV isomer or it is a different isomeric state.

The four transitions with energies of 670, 683, 714, and 728 keV were previously observed and placed in a level scheme [23]. Based on the coincidences between the 787- and 714-keV γ rays, the ordering of the 714- and 683-keV sequence is inverted with respect to Ref. [23].

The inset of Fig. 6 shows a summed time spectrum for the isomeric state in ^{125}Ag and the fit to the slope of the distribution gives a half-life of 474(35) ns for the 1501-keV isomeric state. The half-life, obtained in the present work, overlaps with $t_{1/2} = 473(111)$ ns given in Ref. [23] and with 0.44(9) μs from Ref. [24] and is consistent with 0.498^{+21}_{-20} μs in Ref. [26].

The delayed coincidence method [27] was used to estimate the half-life of the 714- and 670-keV levels. It showed that

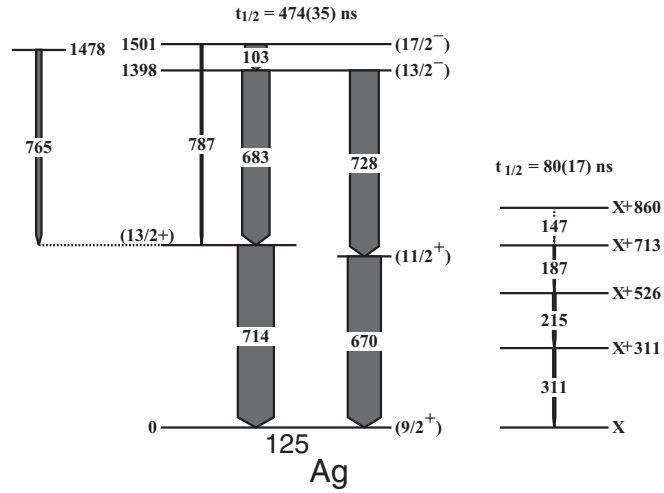

FIG. 8. Partial level scheme of ^{125}Ag, based on the observed γ-ray coincidences.

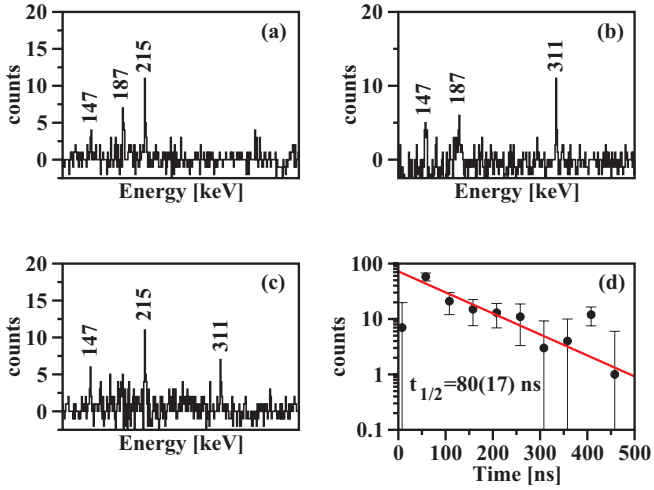

FIG. 9. (Color online) ^{125}Ag γ rays, observed in coincidence with the (a) 311-keV, (b) 215-keV, and (c) 187-keV transition, respectively. (d) A summed time spectrum for the three transitions.

the half-life of the two excited states is shorter than the DGF time binning. This observation is consistent with a dipole or a quadrupole nature of the 714- and 670-keV transitions.

Several weak lines with energies of 74, 129, 155, 187, 215, and 311 keV were observed in coincidence with the ^{125}Ag ions. The 311-, 215-, and 187-keV lines were observed in mutual coincidence and in a tentative coincidence with a weaker 147-keV transition as shown in Figs. 9(a)–9(c). The half-life of 80(17) ns was deduced from the slope of the time spectrum shown in Fig. 9(d). Coincidences between this group of transitions and the transitions deexciting the 474-ns isomer were not observed, which enables the placement of this group of transitions in parallel to the main branch.

The γ-ray energies and intensities are listed in Table II. An intensity imbalance between the 714- and 683-keV transitions

TABLE II. Level energies (E_i), spin/parity (J^π) assignments, γ-ray energies (E_γ), and relative intensities ($I_{\rm rel}$) for transitions, observed in coincidence with the ^{125}Ag ions.

E_i (keV)	J^π	E_γ (keV)	$I_{\rm rel}$ (%)
		74.2(5)[a]	8(1)
		129.3(10)[a]	$\leqslant$1
		155.0(10)[a]	$\leqslant$1
0	$(9/2^+)$		
670	$(11/2^+)$	669.8(5)	90(3)
714	$(13/2^+)$	714.1(5)	100
1398	$(13/2^-)$	683.4(5)	73(3)
		728.3(5)	80(3)
1478		764.5(5)	13.8(16)
1501	$(17/2^-)$	102.5(5)	61.6(20)
		787.0(5)	5.5(12)
X			
$X+311$		310.6(5)	6.0(12)
$X+526$		215.0(5)	8(4)
$X+713$		187.3(5)	3.9(13)
$X+860$		147.0(10)	$\leqslant$1

[a]Not placed in the level scheme.

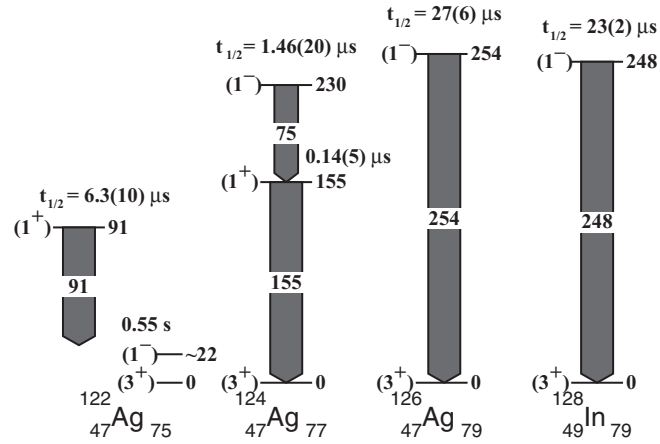

FIG. 10. ^{122,124,126}Ag level schemes compared to the ^{128}In level scheme reported in Ref. [19]. The (1^-) level in ^{122}Ag is from Ref. [32].

was reported in Ref. [23], with the 683-keV transition being the stronger. The analysis, performed in the present work, shows indeed an imbalance of 17%, but in the opposite direction. However, the 765- and 787-keV transitions were also observed in coincidence with the 714-keV transition, helping to balance the intensity for the 714-keV level. The intensity balance for the 1398-keV level suggests that the 103-keV transition is converted with $\alpha = 1.48(8)$, which is close to the theoretical value of 1.3 for an $E2$ transition calculated with BrIcc [30].

In ^{125}Ag, the spin and parity assignments are based on the observed γ-decay pattern, in analogy with ^{123}Ag, and on the systematics presented in Fig. 5. In contrast to the level scheme proposed in Refs. [23,26], $J^\pi = 11/2^+$ was assigned to the lower-lying excited state in ^{125}Ag. For the 1501-keV level, the $B(E2; 17/2^- \rightarrow 13/2^-) = 1.18(11)$ W.u. and $B(M2; 17/2^- \rightarrow 13/2^+) = 3.2(8) \times 10^{-4}$ W.u. values, calculated with $\alpha(103\gamma; E2) = 1.324$ and $\alpha(787\gamma; M2) = 0.0056$ [30], respectively, are consistent with the hindrance factor systematics [31].

B. Even-*A* Ag nuclei

Figure 10 presents the partial level schemes of ^{122}Ag, ^{124}Ag, and ^{126}Ag, obtained in the present work and compared to the odd-odd neighbor ^{128}In [19].

1. ^{122}*Ag*

Prior to our study two isomeric states with half-lives of 0.20 and 0.55 s and $J^\pi = (9-)$ and $(1-)$ were observed in ^{122}Ag [11,32], but no isomeric decay transitions had been seen. The present work reports on a new shorter-lived isomer, observed in the relativistic fission of ^{238}U and the fragmentation of ^{136}Xe. In these experiments the FRS was tuned to transmit ^{120}Rh and ^{126}Cd, respectively.

Figure 11 shows a γ-ray spectrum observed in delayed coincidence with the ^{122}Ag ions within a 8.75-μs-wide time window opened 2.75 μs after implantation. A single γ ray with an energy of 91 keV is observed. The inset of Fig. 11 shows the time distribution of the 91-keV transition. A half-life of $t_{1/2} = 6.3(10)$ μs was obtained from the slope, which

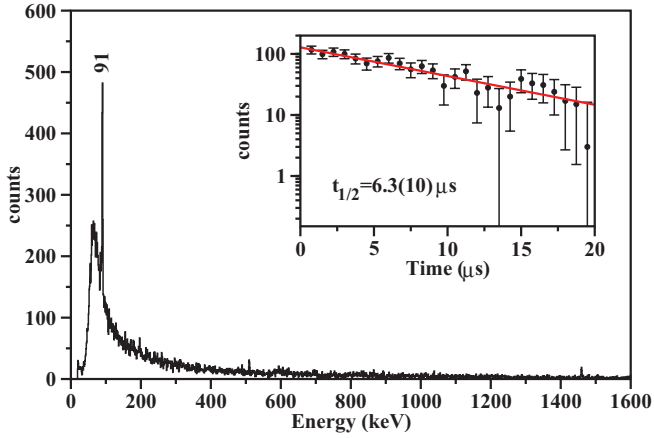

FIG. 11. (Color online) γ-ray energy spectrum observed in coincidence with ^{122}Ag ions. The inset shows the time distribution of the 91-keV transition.

suggests $E1$ or $E2$ multipolarity, given that only $B(E1) = 4.8(8) \times 10^{-8}$ W.u. and $B(E2) = 0.133(23)$ W.u. calculated with $\alpha(91\gamma; E1) = 0.2092$ and $\alpha(91\gamma; E2) = 2.02$ [30] are consistent with the hindrance factor systematics [31].

Similar low-lying μs isomeric states were observed in the neutron-rich ^{126,128,130}In Ref. [19] and related to the decay of the 1^- and 3^+ states. Also, an excited 1^+ state is present in ^{126,128,130}In Ref. [19]. It is 1692 keV above the 3^+ level in ^{130}In and decreases in energy to 688 keV above the 3^+ ground state in ^{126}In. In ^{122}Ag, however, 3^+ is assigned to the ground state [32] on the basis of the log$ft \approx 5.4$ and 5.9 to the daughter $2+$ and $(4+)$ levels, respectively, and (1^-) is assigned to the 0.55-s isomer in Ref. [11]. Therefore, based on the analogy with ^{126,128,128}In, $J^\pi = (1^+)$ was tentatively assigned to the isomeric level observed in the present study. Given that the multipolarity of the 91-keV transition is $E1$ or $E2$, the final state can be the (1^-) excited state or the (3^+) ground state.

The level energy $E(1^-) \approx 22$ keV of the 0.55-s isomer is estimated from its half-life and the $M2$ transition strength in ^{126,128}In Ref. [19]. This enables the placement of the (1^-) state between the (1^+) isomeric state and the ground state of ^{122}Ag.

2. ^{124}Ag

Prior to our study, two γ rays with energies of 155 and 1132 keV were observed in mutual coincidence and associated with ^{124}Ag [24].

In the present work, ^{124}Ag was observed in the ^{120}Rh FRS settings from ^{238}U fission and in the ^{126}Cd and ^{130}Cd FRS settings from fragmentation of the ^{136}Xe beam. Figure 12 shows γ-ray spectra, observed in delayed coincidence with ^{124}Ag nuclei within a 5.75-μs time window opened 450 ns after implantation. Two transitions with energies 75 and 155 keV were observed to be in coincidence. The two γ rays are observed also in Ref. [26]. The 1132-keV line, reported previously in Ref. [24], is not confirmed by the present study. The inset of Fig. 12(a) shows the summed time spectrum for the 75- and 155-keV transitions and the half-life, obtained from the fit to the slope, is 1.46(20) μs, which is consistent with the 1.62^{+29}_{-24} μs in Ref. [26].

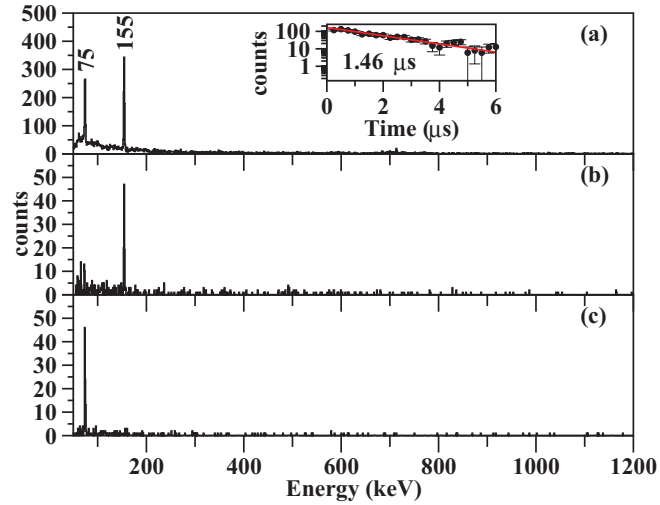

FIG. 12. (Color online) γ-ray energy spectra observed in coincidence with ^{124}Ag ions. (a) Total projection; (b) γ rays in coincidence with the 75-keV transition; (c) γ rays in coincidence with the 155-keV transition; (inset) a summed time spectrum for the 75- and the 155-keV transitions.

The 155-keV γ ray is delayed with respect to the 75-keV γ ray, which enables the ordering made in the level scheme in Fig. 10. However, the two transitions are of low energy and therefore a time-walk correction has to be made to properly determine the half-life of the intermediate state. The time walk of the prompt distribution as a function of the energy was determined by using data for ^{126,128}Cd from [15,33] and for ^{123,125}Ag from the present experiment. Time distributions, calculated as the difference $T = t_1 - t_2$ between the detection time of the feeding t_1 and deexciting t_2 transitions, were analyzed. The centroids of the prompt distribution were obtained for several transitions in ^{126,128}Cd and ^{123,125}Ag, where the level of interest is fed by a low-energy transition and deexcited by a high-energy transition. The centroid of the time distribution is plotted on Fig. 13 as a function of the low-energy feeding transition. The energy-time dependence was fitted with a function of the type $T(E_\gamma) = a/E_\gamma + b$, where T is the centroid of the time distribution, E_γ is the energy of the feeding transition in keV and $a = 172\,28$ ns·keV,

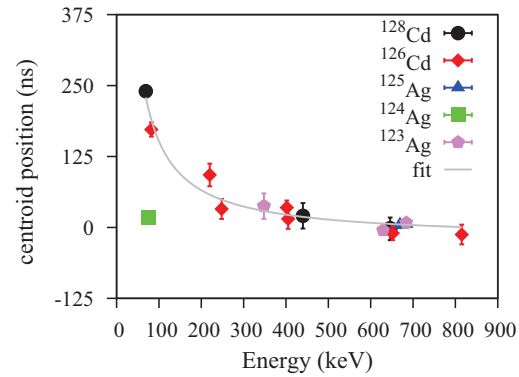

FIG. 13. (Color online) Time-walk correction for the Ge detectors. Details about the ^{124}Ag data point are presented in the text.

TABLE III. Decay properties of the isomeric state in ^{124}Ag. Level energy (E_i), half-life ($T_{1/2}$), γ-ray energy (E_γ), relative intensity (I_γ), and the experimental total conversion γ-ray coefficient (α_{exp}) obtained for the 75-keV transition and compared to the theoretical total conversion coefficients (α_{th}) calculated for $E1$, $M1$, $E2$, and $M2$ multipolarities.

E_i (keV)	$T_{1/2}$ (μs)	E_γ (keV)	I_γ (%)	α_{exp}	α_{th} $E1$	α_{th} $M1$	α_{th} $E2$	α_{th} $M2$
230	1.46	75	74(38)	0.4(8);0.8(9)	0.36	0.95	4.0	13
155	0.14	155	100(16)		0.05	0.12	0.30	0.89

$b = -20.6$ ns are the parameters obtained from the fit. A mirror symmetric function [34] for the position of the prompt distribution can be obtained from a set of states fed by a high-energy transition and decaying via a low-energy transition. In the ^{124}Ag case, the two transitions have low energies. Therefore, the ^{124}Ag data point was plotted on Fig. 13 after time-walk correction was applied for the 75-keV feeding transition. Thus, a half-life of 0.14(5) μs was obtained from the difference between the ^{124}Ag data point and the $T(E_\gamma)$ value for $E_\gamma = 155$ keV. The $B(E1) = 5.0(18) \times 10^{-7}$ W.u. and $B(E2) = 0.9(4)$ W.u. values, calculated for the 155-keV transition with $\alpha(155\gamma; E1) = 0.0457$ and $\alpha(155\gamma; E2) = 0.303$ [30], are consistent with the systematics [31]. An $M1/E2$ multipolarity assignment for the 155-keV transition is also possible for $\delta \leqslant 0.1$.

Table III shows that the 75-keV transition has an intensity of 74(38)% of that of the 155-keV transition. The intensity balance for the 155-keV level leads to $\alpha(75\gamma) = 0.4(8)$ in case of pure $E1$ 155-keV transition and to $\alpha(75\gamma) = 0.8(10)$ if 155-keV transition is a pure $E2$ transition. These conversion coefficients are consistent with an $E1$ nature of the 75-keV transition. Thus, $B(E1) = 3.2(5) \times 10^{-7}$ W.u. was obtained with $\alpha(75\gamma; E1) = 0.363$.

Because $J^\pi \geqslant 2$ was assigned to the ground state of ^{124}Ag [35] and given no other experimental data is available, the spin/parity assignments to the levels in ^{124}Ag are based on analogy with ^{122}Ag and the systematics for the neutron-rich indium nuclei [19].

3. ^{126}Ag

^{126}Ag is the most neutron-rich nucleus in the silver isotopic chain studied in the present experiment. The ions were transmitted through the FRS in the ^{130}Cd setting during the ^{136}Xe beam fragmentation experiment. The energy spectrum, shown on Fig. 14, was incremented for delayed transitions in coincidence with the ^{126}Ag ions within a 48-μs-wide time window placed 0.58 μs after the prompt-γ flash. A single γ ray at energy of 254 keV was detected by RISING. The inset of the figure presents the time distribution of the 254-keV line and a half-life of 27(6) μs was obtained from the slope. The isomeric transition in ^{126}Ag is also reported in Ref. [26] and a lower limit of the half-life is given to be 20 μs.

An $M2$ multipolarity assignment for the isomeric transition is based on comparison between the measured half-life with the Weisskopf estimates for the partial half-life of a 254-keV transition, and the hindrance factor systematics for low-lying

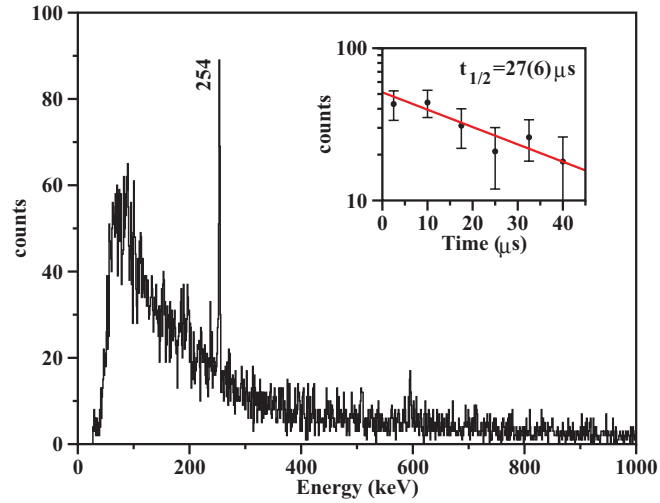

FIG. 14. (Color online) γ-ray energy spectrum observed in delayed coincidence with the ^{126}Ag ions. (Inset) Time spectrum gated on the 254-keV transition.

transitions in the mass region $100 < A < 132$ [31]. $B(M2) = 0.037(9)$ W.u. is calculated with $\alpha(254\gamma; M2) = 0.1645$ [30]. The $M2$ nature of the isomeric transition is also consistent with the isomeric decay in the $^{128}_{49}$In$_{79}$ isotone as shown in Fig. 10, where the $J^\pi = (1^-)$, $t_{1/2} = 23$ μs isomer decays via a 248-keV $M2$ transition to the (3^+) ground state with $B(M2) = 0.047(5)$ W.u. Therefore, (1^-) and (3^+) are assigned to the 254-keV and the ground state levels in ^{126}Ag.

IV. DISCUSSION

A. odd-*A* Ag nuclei

The systematics, presented in Fig. 5, show that the level energies in the odd-mass silver nuclei evolve smoothly with the neutron number following the trend of the first 2^+ level of the Cd core. Often, such states are interpreted as core coupled states.

Based on the relative positioning of the $7/2^+$ level with respect to the $9/2^+$ level, two groups of nuclei can be distinguished. For $N \leqslant 54$ the $7/2^+$ level energy is higher than the $9/2^+$ level energy. For $N > 54$ the relative positioning of the two levels inverts. Extrapolating the trend towards $N = 82$, it can be expected that $9/2^+$ becomes the ground state again. While the group of nuclei with less then six valence particles or holes can be understood in the single-particle framework the anomalous position of the $j - 1 = 7/2$ state hints at a more complex structure.

The origin of this anomaly was initially related to the three-proton cluster configuration [36]. Having 47 protons, the only available proton subshell for the silver valence proton holes is $1g_{9/2}$. Also, given that this is a unique-parity orbit, the low-lying positive parity states can arise only from the $\pi g_{9/2}^{-3}$ configuration. By using the expansion coefficients of the three-particle matrix elements of a two-body interaction in terms of two-particle matrix elements for the $\{j^{-3}\}$ configuration of identical nucleons [37], energy spectra were calculated for the $^{97-129}_{47}$Ag$_{50-82}$ isotopes. Figure 15 shows the energy spectra,

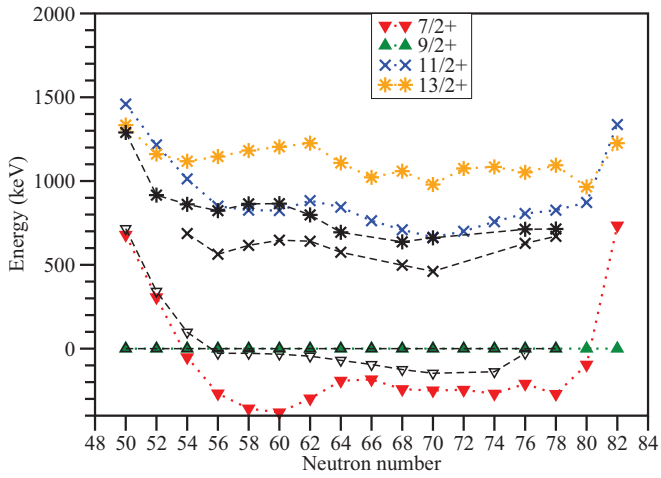

FIG. 15. (Color online) Evolution of the $\pi g_{9/2}^{-3}$ cluster in odd-A Ag nuclei. The theoretical level energies are plotted with colored symbols and compared to the experimental level energies in black. The same symbols are used for theoretical and experimental levels of a given spin and parity.

obtained from

$$\langle j^3\alpha; JM|H|j^3\alpha; JM\rangle = 3\sum_{J'}[j^2(J')jJ|\}j^3J]^2 A_{J'}, \quad (1)$$

where $A_{J'}$ are the two-body matrix elements, parametrized with respect to the neighboring even-even cadmium nuclei, and $[j^2(J')jJ|\}j^3J]$ are the coefficients of fractional parentage listed in Ref. [38]. With the exception of ^{101}Ag$_{54}$ and ^{125}Ag$_{78}$, this simple approach gives a good overall description of the experimental data and in particular it reproduces correctly the sequence of the levels, hinting at the importance of the $\pi g_{9/2}^{-3}$ cluster configuration in understanding the structure of the silver nuclei. However, the systematics in Fig. 15 show also that the theoretical $11/2^+$ and $13/2^+$ level energies are systematically overestimated and the description of the $7/2^+$ level energy in $^{103-109}_{47}$Ag$_{56-62}$ and in $^{123}_{47}$Ag$_{76}$ is poor. Moreover, the negative-parity $13/2^-$ and $17/2^-$ levels in ^{123,125}Ag are outside the model space. A more realistic description of the excited states in the odd-mass silver isotopes, and in ^{123,125}Ag nuclei in particular, should include a larger space and a certain degree of collectivity. A small quadrupole deformation was suggested already at ^{101}Ag$_{54}$ to account for the $E3$ isomeric transition strength between the $1/2^-$ and $7/2^+$ states [39]. Further away from the $N = 50$ magic number rotational bands based on the $\pi 7/2^+[413]$ Nilsson orbit appear [40]. As the $N = 82$ magic number is approached, a reduction of collectivity should take place and the excited states are expected to have purer wave functions.

Given that the above approach does not take into account the proton-neutron and neutron-neutron interactions, which are important in the midshell and transitional regions, shell-model calculations were performed for the $^{123-129}$Ag odd-even nuclei using the NUSHELL code [41]. The full jj45pn space, involving $1f_{5/2}$, $2p_{3/2}$, $2p_{1/2}$, $1g_{9/2}$ proton and $1g_{7/2}$, $2d_{5/2}$, $2d_{3/2}$, $3s_{1/2}$, $1h_{11/2}$ neutron orbitals was used. The theoretical spectra, shown in Fig. 16, are obtained with the jj45pna

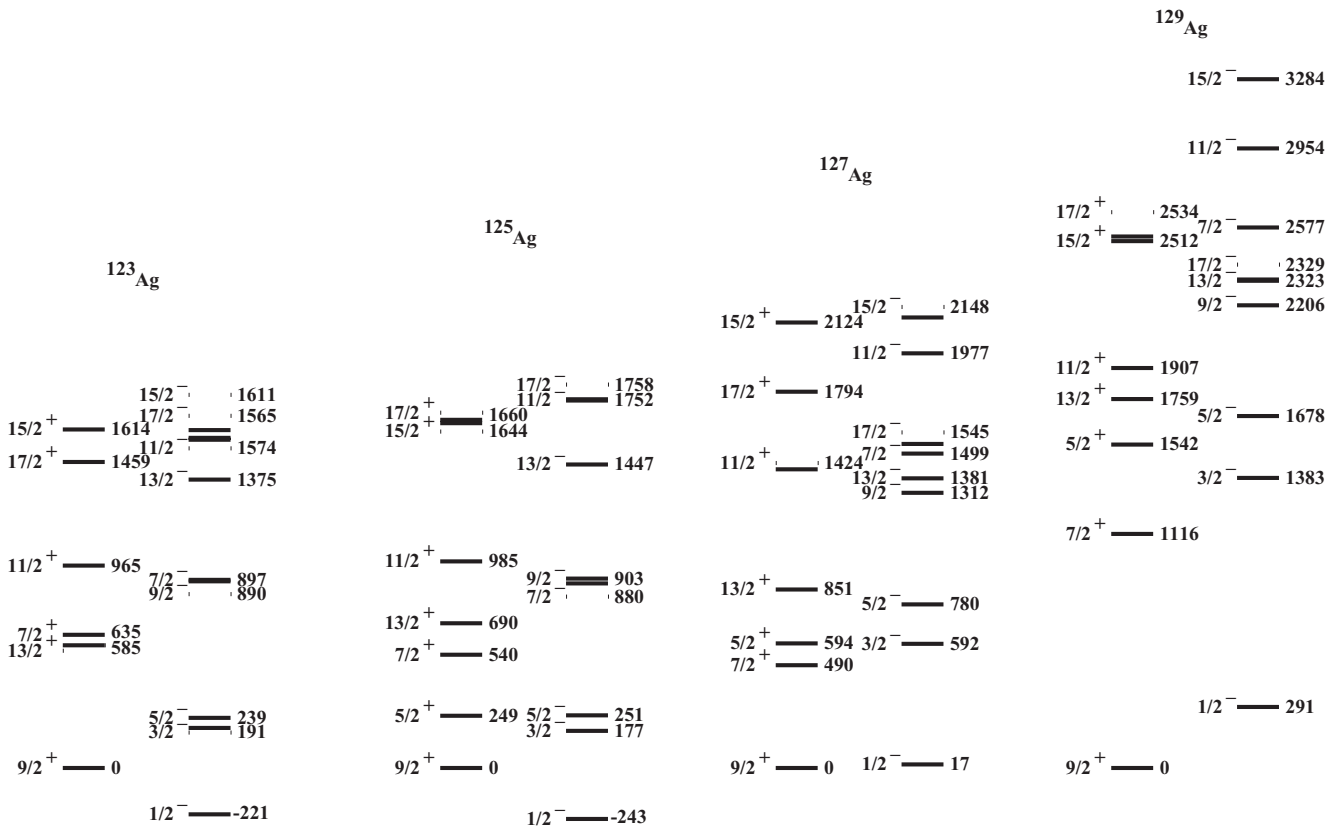

FIG. 16. The results of shell-model calculations for ^{123,125,127,129}Ag, obtained with the jj45pna interaction.

interaction, parametrized with respect to the nuclei lying close to the doubly magic ^{132}Sn. The theoretical level energies evolve smoothly from ^{129}Ag to ^{123}Ag, predicting the $9/2^+$ state to be the lowest-lying positive-parity state. In ^{129}Ag, the wave function of the $J^\pi = 9/2^+$ ground state and the $J^\pi = 11/2^+ - 17/2^+$ yrast states consist of almost pure $\pi 1g_{9/2}^{-3}$ configuration with an amplitude of 68% for the ground state. In the lighter ^{123,125}Ag the respective wave functions are more fragmented, because of the larger valence space. Even though the positive parity states observed in ^{123,125}Ag are present in the calculated level schemes, their sequence is incorrect. In particular, the $7/2^+$ level energy in ^{123}Ag appears 635 keV above the $9/2^+$ state and the ordering of the $11/2^+$, $13/2^+$ doublet is opposite to the experimental level scheme. Also, the energies of the isomeric $17/2^-$ and $13/2^-$ levels in ^{123,125}Ag are overestimated by NUSHELL by 300 to 500 keV. Similar deviations from the experimental data were observed also in the neutron-rich indium isotopes [19]. The shell model with the jj45pna interaction and $e_p = 1.35$ and $e_n = 0.78$ effective charges gives an overestimated $B(E2; 17/2^- \to 13/2^-) =$ 18.5 W.u. value for the isomeric 48-keV transition in ^{123}Ag with respect to the experimentally observed 6.8(8) W.u. given in Sec. III A1.

A different theoretical approach was given many years ago by a model where a cluster of three valence protons was coupled to quadrupole vibrations [42]. In these calculations, the particles are allowed to move in the $\pi g_{9/2}$, $\pi p_{1/2}$, and $\pi p_{3/2}$ subshells and are coupled to a Sn vibrational core. Even though there are no specific calculations for the neutron-rich silver isotopes, a qualitative analysis can be made given that the even-even medium-mass cadmium nuclei have a smooth behavior with their first phonon being at approximately 500–600 keV. A good overall description of the medium-mass silver nuclei, where the $j-1$ anomaly takes place, can be obtained with a coupling parameter strength $a \geqslant 0.7$. The energy levels were calculated in Ref. [42] for the negative parity states up to $19/2_1^-$ and for the positive-parity states up to $13/2_1^+$. The $7/2_1^+$ level has a seniority $v = 3$ zero-phonon and one-phonon component, as well as a $v = 1$ one-phonon contribution, each with an amplitude of approximately 20%. The $9/2_1^+$ level has a dominant contribution of the $v = 1$ zero-phonon component with an amplitude of 30% and a $v = 3$ one-phonon component with a contribution of 17%. The $11/2^+$ state is more fragmented with $v = 3$ zero-phonon, $v = 1$ one-phonon, and $v = 2$ two-phonon components with amplitudes of 16%, 21%, and 12%, respectively. For the $13/2^+$ state, the components with amplitudes higher than 10% are the $v = 3$ zero-phonon and the $v = 1$ one-phonon components.

The model calculations give $B(E2; 17/2_1^- \to 13/2_1^-) =$ 18.4 W.u. or 16.0 W.u. values for the 48-keV isomeric transition in ^{123}Ag, obtained with two sets of effective charges $e_{\rm eff}^{\rm s.p.} = 2$ and $e_{\rm eff}^{\rm vib} = 2$ and 2.5. Both values overestimate the experimental one. Nevertheless, the model gives a good qualitative description of the level sequence and the multiplet structure in particular, hinting at the importance of zero- and one-phonon excitations in understanding the structure of the lowest-lying positive-parity yrast states.

In the low-spin regime, the cluster-vibration and the shell model predict different transition strengths. The shell-model calculations give $B(E2, 9/2_1^+ \to 7/2_1^+) = 4.8$ W.u. for the 27-keV transition in ^{123}Ag, while the cluster-vibration model predicts a more enhanced transition with $B(E2, 9/2_1^+ \to 7/2_1^+) = 27.5$ W.u. Even though the present experiment does not allow the measurement of the half-life and the mixing ratio of the 27-keV transition in ^{123}Ag, the models have clear predictions which can be tested in future experiments.

B. Even-*A* Ag nuclei

The low-lying excited states in the odd-odd neutron-rich silver nuclei can be described by using the cluster-vibration model, where the proton-neutron residual interaction is a result of quadrupole and spin vibration phonon exchange between the odd particles and the nuclear core [10]. As a result, split multiplets with level energies $E[(j_p, j_n)J]$ as a function of the nuclear spin J arise. The level energies obey the parabolic rule

$$E[(j_p, j_n)J] = E_{j_p} + E_{j_n} + \delta E_2 + \delta E_1, \tag{2}$$

where the quadrupole δE_2 and spin-vibrational δE_1 contributions to the splitting of the multiplet are given by

$$\begin{aligned}
\delta E_2 &= -\alpha_2 \mathscr{V} \frac{[J(J+1) - j_p(j_p+1) - j_n(j_n+1)]^2 + J(J+1) - j_p(j_p+1) - j_n(j_n+1)}{2j_p(2j_p+2)2j_n(2j_n+2)} + \mathscr{V}\frac{\alpha_2}{12}, \\
\delta E_1 &= -\alpha_1 \xi \frac{J(J+1) - j_p(j_p+1) - j_n(j_n+1)}{(2j_p+2)(2j_n+2)}.
\end{aligned} \tag{3}$$

Here, E_{j_p} and E_{j_n} denote the quasiproton $|j_p\rangle$ and the quasineutron $|j_n\rangle$ energies and are deduced from the experimental data. j_p and j_n are the proton and neutron total angular momenta, and $J = |j_p - j_n|, \ldots, (j_p + j_n)$ is the nuclear total angular momentum. If $|j_p\rangle$ and $|j_n\rangle$ are both particlelike or both holelike the parameter $\mathscr{V} = 1$; otherwise, $\mathscr{V} = -1$. The parameter ξ is defined as $\xi = 1$ if the Nordheim number $\mathscr{N} = j_p - l_p + j_n - l_n = -1$ and $\xi = (2j_p+2)(2j_n+2)/(2j_p 2j_n)$ if $\mathscr{N} = 1$. Otherwise, $\xi = -(2j_p+2)/2j_p$ for $\mathscr{N} = 0^-$ and $\xi = -(2j_n+2)/2j_n$ for $\mathscr{N} = 0^+$, where the symbols $\mathscr{N} = 0^-$ and $\mathscr{N} = 0^+$ distinguish the cases $j_n - l_n = -1/2$, $j_p - l_p = 1/2$ and $j_n - l_n = 1/2$, $j_p - l_p = -1/2$. The quadrupole and spin vibration coupling strengths are defined as

$$\begin{aligned}
\alpha_2(j_p, j_n) &= \alpha_2^{(0)} \left| \left(U_{j_p}^2 - V^2 j_p\right)\left(U_{j_n}^2 - V_{j_n}^2\right) \right|, \\
\alpha_1(j_p, j_n) &= \alpha_1^{(0)},
\end{aligned} \tag{4}$$

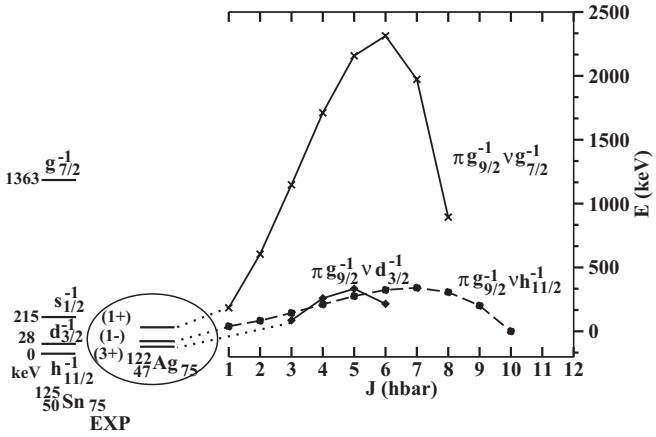

FIG. 17. Proton-neutron quasiparticle multiplets in ^{122}Ag. Neutron single-particle states in ^{125}Sn are taken from Ref. [44].

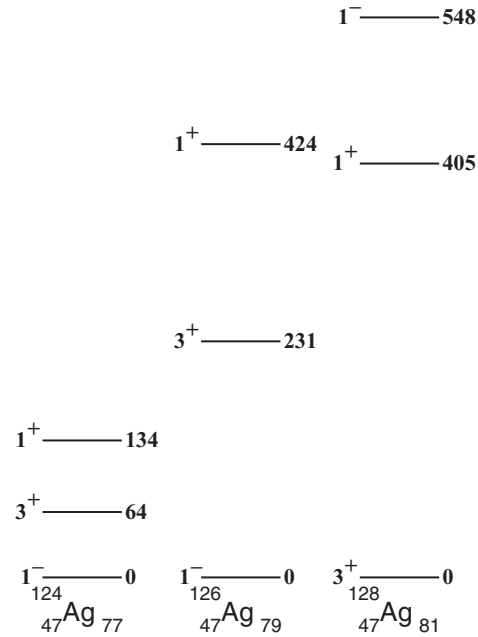

FIG. 18. Partial theoretical level schemes for $^{122-128}$Ag obtained with the jj45pna interaction.

where V_j^2 is the occupation probability for the level j and $U_j^2 = 1 - V_j^2$.

This approach was used extensively in the midshell indium isotopes [43], where a good overall agreement with the experimental data was achieved. The level energies of ^{122}Ag were calculated by using the single-particle neutron energies taken from the ^{125}Sn$_{75}$ level scheme [44], which is presented in Fig. 17. The neutron occupation probabilities, listed in Table IV, were calculated from the spectroscopic factors S, obtained in the ^{124}Sn$(d, p)^{125}$Sn$_{75}$ reaction [45]. The coupling strengths $a_1^{(0)} \approx 15/A = 0.12$ MeV and $a_2^{(0)} = 382\beta_2^2(\hbar\omega_2)^{-1} = 16.23$ MeV were deduced from the β_2 and the E_{2^+} energy of the first phonon excitation in ^{124}Cd. The proton occupation probability $V(\pi 1g_{7/2})^2 = 0.80$ is deduced from Ref. [46].

Figure 17 shows the calculated parabolas for the $\pi g_{9/2}^{-1} \otimes \nu g_{7/2}^{-1}$, $\pi g_{9/2}^{-1} \otimes \nu d_{3/2}^{-1}$, and $\pi g_{9/2}^{-1} \otimes \nu h_{11/2}^{-1}$ multiplets in ^{122}Ag. Within each of the multiplets, the excited states decay via fast $M1$ transitions, and hence the observed isomeric states can arise only from transitions connecting states of different multiplets. The lowest-lying states, belonging to each of the multiplets, are the 1^-, 3^+, and 1^+ states, which is consistent with the experimental data.

Shell-model calculations were also performed for $^{122-128}$Ag with the full jj45pn space. Results are presented in Fig. 18. In ^{128}Ag, the main component of the 1^+ wave function (w.f.) is $\pi g_{9/2}^{-1} \otimes \nu g_{7/2}^{-1}$ with an amplitude of 30%, followed by $\pi p_{1/2}^{-2} \otimes \nu g_{7/2}^{-1}$ with 10%. The w.f. of the 3^+ state has a leading $\pi g_{7/2}^{-1} \otimes \nu d_{3/2}^{-1}$ component with an amplitude of 39%. Weaker components are $\pi p_{1/2}^{-2} \otimes \nu d_{3/2}^{-1}$ and $\pi p_{3/2}^{-2} \otimes \nu d_{3/2}^{-1}$ with 13% and 11%, respectively. The 1^- state consists of $\pi g_{9/2}^{-1} \otimes \nu h_{11/2}^{-1}$, contributing 34% of the w.f., and $\pi p_{1/2}^{-2} \otimes \nu h_{11/2}^{-1}$ which has an amplitude of 24% of the w.f. All other components contribute with smaller amplitudes. In the lighter nuclei, these configurations become diluted and the wave functions are much more fragmented. The relative position of the theoretical 1^+ and 3^+ is the same as the ordering of the experimental levels. However, in contrast to the spin/parity assignments made in the present work, the theoretical 1^- is pushed below the 3^+ states in ^{124,126}Ag. The behavior of the 1^- level in the neutron-rich even-even Ag nuclei is not surprising, because in the neutron-rich even-A indium nuclei a strong variation of the 1^- state with respect to the 3^+ state is also observed and attributed to a weakening of the effects of the p-n interaction when moving from ^{129}In$_{82}$ to ^{126}In$_{78}$ [19]. It was suggested also that the underestimation of the p-n interaction in the region of nuclei with $N < 82$ may limit the predictive power of the shell model.

TABLE IV. Spin and parities (J^π), level energies (E), configurations, spectroscopic factors [45] (S), and neutron occupation probabilities (V_k^2) for ^{125}Sn$_{75}$.

J^π	E (keV)	Configuration	S	V_k^2
$11/2^-$	0	$\nu 1h_{11/2}$	0.42	0.58
$3/2^+$	28	$\nu 2d_{3/2}$	0.44	0.56
$1/2^+$	215	$\nu 3s_{1/2}$	0.33	0.67
$7/2^+$	1363	$\nu 1g_{7/2}$	0.038	0.96

V. CONCLUSIONS

This work presents results on two previously known submicrosecond isomers and on two new isomeric states in ^{123,125}Ag. Because of the high efficiency and granularity of RISING, coincidences were established enabling the construction of the level schemes. A new microsecond isomer was observed in ^{122}Ag. The isomeric state in ^{124}Ag is observed to decay via a 75-keV transition and a half-life of the intermediate state was deduced. An isomeric state with a half-life of 27(6) μs is observed in ^{126}Ag. The spin/parity assignments are based on the systematics and the observed decay pattern.

The positive-parity states of the odd-mass nuclei were analyzed within a $\pi g_{9/2}^{-3}$ coupling scheme, based on a simple angular momentum recoupling algebra, and the results compared to shell-model calculations, performed in a larger space. A reasonable description of the isomeric $17/2^-$ and the $13/2^-$ level energies is achieved. The biggest discrepancy between the theoretical calculations and the ^{123}Ag data is in the $7/2^+$ level energy, which appears 635 keV above the ground state. In ^{123,125}Ag, the theoretical level energy for the $11/2^+$ is also overestimated by approximately 300 keV. Further qualitative analysis was made in the framework of the cluster-vibration model.

The excited states in the even-mass silver nuclei were analyzed with the shell model and within a phenomenological approach based on a quadrupole and spin-vibrational proton-neutron interaction.

Even though the phenomenological approaches used in the present work give a satisfactory description of particular levels, more realistic calculations using a larger valence space fail in reproducing the level energy sequence in several cases. This may be explained by an inapplicability of the *p-n* interaction parametrized with respect to the nuclei placed close to ^{132}Sn and by a certain degree of collectivity presented in the nuclei with few valence holes to the $N = 82$ and $Z = 50$ magic numbers. Nevertheless, the intruder $\pi g_{9/2}$ and $\nu h_{11/2}$ orbits seem to play an important role in understanding the structure of the neutron-rich silver nuclei and the isomerism in $^{122-126}$Ag in particular.

ACKNOWLEDGMENTS

This work is supported by the Bulgarian National Science Fund under Contract No. DMU02/1, UK STFC, Royal Society, the Spanish Ministerio de Ciencia e Innovación under Contracts No. FPA2009-13377-C02-02 and No. FPA2011-29854-C04-01, the Spanish Consolider-Ingenio 2010 Programme CPAN (CSD2007-00042), the Swedish Science Council, and OTKA Contract No. K100835.

[1] M. Goeppert-Mayer, Phys. Rev. **74**, 235 (1948); **78**, 16 (1949).
[2] J. Dobaczewski, I. Hamamoto, W. Nazarewicz, and J. A. Sheikh, Phys. Rev. Lett. **72**, 981 (1994).
[3] M. M. Sharma and A. R. Farhan, Phys. Rev. C **65**, 044301 (2002).
[4] W.-T. Chou, R. F. Casten, and N. V. Zamfir, Phys. Rev. C **51**, 2444 (1995).
[5] B. Pfeiffer, K.-L. Kratz, and F.-K. Thielemann, Z. Phys. A **357**, 235 (1997).
[6] I. Dillmann *et al.*, Phys. Rev. Lett. **91**, 162503 (2003).
[7] A. Jungclaus *et al.*, Phys. Rev. Lett. **99**, 132501 (2007).
[8] S. Lalkovski and P. Van Isacker, Phys. Rev. C **79**, 044307 (2009).
[9] T. Sumikama *et al.*, Phys. Rev. Lett. **106**, 202501 (2011).
[10] V. Paar, Nucl. Phys. A **331**, 16 (1979).
[11] K.-L. Kratz, B. Pfeiffer, F.-K. Thielemann, and W. B. Walters, Hyperfine Interact. **129**, 185 (2000).
[12] J. A. Pinston, C. Foin, J. Genevey, R. Béraud, E. Chabanat, H. Faust, S. Oberstedt, and B. Weiss, Phys. Rev. C **61**, 024312 (2000).
[13] R. Lozeva *et al.*, Phys. Rev. C **77**, 064313 (2008).
[14] S. Pietri *et al.*, Phys. Rev. C **83**, 044328 (2011).
[15] L. Cáceres *et al.*, Phys. Rev. C **79**, 011301 (2009).
[16] F. Naqvi *et al.*, Phys. Rev. C **82**, 034323 (2010).
[17] M. Górska *et al.*, Phys. Lett. B **672**, 313 (2009).
[18] P. H. Regan, Int. J. Mod. Phys. E **17**, 8 (2008).
[19] A. Scherillo *et al.*, Phys. Rev. C **70**, 054318 (2004).
[20] A. M. Bruce *et al.*, Phys. Rev. C **82**, 044312 (2010).
[21] H. Geissel, Nucl. Instr. Methods Phys. Res. B **70**, 286 (1992).
[22] S. Pietri *et al.*, Nucl. Instr. Methods B **261**, 1079 (2007).
[23] I. Stefanescu *et al.*, Eur. Phys. J. A **42**, 407 (2009).
[24] B. E. Tomlin, Ph.D. thesis, Michigan State University, 2006.
[25] S. Lalkovski *et al.*, Rutherford Centennial Conference Manchester, UK, 2011 (unpublished).
[26] D. Kameda *et al.*, Phys. Rev. C **86**, 054319 (2012).
[27] W. Andrejtscheff *et al.*, Nucl. Instrum. Methods Phys. Res. **204**, 123 (1982).
[28] D. De Frenne, Nucl. Data Sheets **110**, 2081 (2009).
[29] S. Ohya, Nucl. Data Sheets **102**, 547 (2004).
[30] T. Kibédi, T. W. Burrows, M. B. Trzhaskovskaya, P. M. Davidson, C. W. Nestor Jr., Nucl. Instrum. Methods Phys. Res., Sect. A **589**, 202 (2008).
[31] S. Lalkovski *et al.*, J. Phys.: Conf. Ser. **366**, 012029 (2012).
[32] T. Tamura, Nucl. Data Sheets **108**, 455 (2007).
[33] N. Hoteling *et al.*, Phys. Rev. C **76**, 044324 (2007).
[34] J. M. Régis, G. Pascovici, J. Jolie, and M. Rudigier, Nucl. Instrum. Methods Phys. Res., Sect. A **622**, 83 (2010).
[35] J. Katakura and Z. D. Wu, Nucl. Data Sheets **109**, 1655 (2008).
[36] L. S. Kisslinger, Nucl. Phys. **78**, 341 (1966).
[37] K. Heyde, *The Nuclear Shell Model* (Springer-Verlag, Berlin, 1994).
[38] I. M. Band and Yu. I. Kharitonov, Nucl. Data Tables **10**, 107 (1971).
[39] V. R. Casella, J. G. Knight, and R. A. Nauman, Nucl. Phys. A **239**, 83 (1975).
[40] J. K. Hwang *et al.*, Phys. Rev. C **65**, 054314 (2002).
[41] B. A. Brown *et al.*, MSU NSCL Report, No. 1289, 2004.
[42] V. Paar, Nucl. Phys. A **211**, 29 (1973).
[43] T. Kibédi *et al.*, Phys. Rev. C **37**, 2391 (1988).
[44] J. Katakura, Nucl. Data Sheets **112**, 495 (2011).
[45] C. R. Bingham and D. L. Hillis, Phys. Rev. C **8**, 729 (1973).
[46] S. Y. Van Der Werf, B. Fryszczyn, L. W. Put, and R. H. Siemssen, Nucl. Phys. A **273**, 15 (1976).